

UVR-induced photoinhibition of summer marine phytoplankton communities from Patagonia

Virginia E. Villafañe · Paul J. Janknegt · Marco de Graaff · Ronald J. W. Visser · Willem H. van de Poll · Anita G. J. Buma · E. Walter Helbling

Received: 1 April 2008 / Accepted: 29 April 2008 / Published online: 3 June 2008
© Springer-Verlag 2008

Abstract During austral summer 2006, experiments were carried out to evaluate the effects of ultraviolet radiation (UVR, 280–400 nm) on carbon fixation of natural phytoplankton assemblages from Patagonia (Argentina). Surface water samples were collected (ca. 100 m offshore) at mid morning using an acid-cleaned (1 N HCl) dark container. The short-term impact of UVR (measured as radiocarbon incorporation) was immediately assessed by exposing samples to three artificial illumination treatments: PAR (400–700 nm), PAR + UV-A (320–700 nm), and PAR + UV-A + UV-B (280–700 nm). Pico-nanoplankton characterized the assemblages, and taxon-specific pigment fingerprinting combined with CHEMTAX and supplemented with microscopic observations showed varied proportions of diatoms, chlorophytes, and cyanobacteria throughout January–February 2006. Photosynthetic efficiency, as assessed through assimilation numbers, was high [between 4.4 and 10.4 $\mu\text{g C} (\mu\text{g chl-a})^{-1} \text{h}^{-1}$], and it was probably favored by the supply of inorganic nutrients from the Chubut River. UVR-induced photoinhibition appeared to be related to the taxonomic composition: in general,

higher photoinhibition was observed when diatoms dominated, whereas this was lower when samples were dominated by chlorophytes. Our data suggest that xanthophyll pigments might have provided only limited protection in these already highlighted acclimated assemblages.

Introduction

Phytoplankton organisms rely on solar radiation to drive photosynthesis to synthesize carbohydrates. However, this requirement exposes them also to solar ultraviolet radiation (UVR, 280–400 nm), which is known to affect key molecules, organelles, and metabolic processes (Vernet 2000; Villafañe et al. 2003; Häder et al. 2007). UVR can cause photoinhibition, a process that is variable among species and habitats (Villafañe et al. 2003). Moreover, the effect of UVR depends on nutrient and light history of the algae. For example, significant variability in UVR-mediated photoinhibition was observed when the dinoflagellates *Prorocentrum micans* and *Heterocapsa triquetra* were exposed to solar radiation under different nutrient regimes (Marcoval et al. 2007). Additionally, inhibition of photosynthesis during excessive PAR (photosynthetically active radiation, 400–700 nm) and UVR exposure was influenced by acclimation to low irradiance and high irradiance in two *Thalassiosira* species (van de Poll et al. 2006).

Phytoplankton have developed a suite of physiological and biochemical responses that minimize the negative effects of UVR exposure (Roy 2000; Banaszak 2003). These include the following: (1) reduction of UVR exposure by migrating downward in the water column, as seen in the chlorophyte *Dunaliella salina* (Richter et al. 2007); (2) protection by synthesizing compounds such as mycosporine

Communicated by U. Sommer.

V. E. Villafañe (✉) · E. Walter Helbling
Estación de Fotobiología Playa Unión y Consejo Nacional de Investigaciones Científicas y Técnicas (CONICET),
Casilla de Correos No. 15, 9103 Rawson, Chubut, Argentina
e-mail: virginia@efpu.org.ar

P. J. Janknegt · M. de Graaff · R. J. W. Visser ·
W. H. van de Poll · A. G. J. Buma
Department of Ocean Ecosystems,
Centre for Ecological and Evolutionary Studies,
University of Groningen, P.O. Box 14,
9750 AA Haren, The Netherlands

like amino acids (MAAs) as demonstrated for many species of cyanobacteria, dinoflagellates, and diatoms (Banaszak 2003), and xanthophyll pigments that can potentially dissipate excessive energy as heat (Demming-Adams 1990; Demers et al. 1991; Sobrino et al. 2005); and (3) repairing DNA and/or protein damage (Buma et al. 2003; Bouchard et al. 2005).

The net UVR impact in natural microbial communities is the result of species specific differences in sensitivity as well as in acclimation potential. Because of seasonal shifts in species dominance and abundance, together with nutrient and irradiance levels, it can be expected that the overall UVR impact on phytoplankton also shows seasonal variation. A study carried out with natural phytoplankton communities from coastal Patagonian waters demonstrated interseasonal variability of UVR effects, with high UVR-induced photoinhibition during spring and summer, and low levels during winter (Villafañe et al. 2004). However, biological weighting functions for this process showed that winter communities were more sensitive than those characterizing the summer. On the other hand, another study (Banaszak and Neale 2001) showed that phytoplankton in the Rhode River had a moderate sensitivity towards UVR that mainly varied on short-term rather than on seasonal time scales. In addition, a study in the Great Lakes demonstrated that, in spite of the large variations in nutrients and irradiance, phytoplankton sensitivity towards UVR was similar throughout the year (Furgal and Smith 1997). Finally, Gao et al. (2007) showed that the size structure of the community and cloudiness conditioned the overall impact of UVR on phytoplankton photosynthesis in a tropical marine site of Southern China. Thus, responses to UVR stress are not only related to the differential sensitivity of the sampled assemblages, but also to the combination of UVR exposure with other environmental variables.

The focus of our study was to obtain knowledge on the variability of UVR effects on photosynthesis of summer phytoplankton communities of Patagonian coastal waters with a resolution of 2–3 days. To achieve this, we evaluated the shifts in phytoplankton community composition by means of HPLC pigment fingerprinting in combination with the CHEMTAX program, as well as by classical microscopy and size fractionation. Then, we studied the effects of UVR on carbon incorporation using short-term artificial UVR exposures by means of a solar simulator. In this way, possible effects of variable exposure quantity and quality (as caused by season, time of day, atmospheric influences) were eliminated. In addition, we assessed the importance of photoprotective mechanisms (xanthophyll cycling) that would allow these communities to cope with the normally high radiation levels as registered in the area at this time of the year (Helbling et al. 2005).

Materials and methods

Study area and sampling

This study was conducted at Bahía Engaño, Chubut, Argentina (43°18.8'S, 65°02'W, Fig. 1) during the period from January 10, 2006, to February 19, 2006. The study site is located in close proximity to the Chubut River estuary, where geomorphology, biological, and chemical characteristics were studied previously (Perillo et al. 1989; Villafañe et al. 1991; Helbling et al. 1992; Sastre et al. 1994; Commendatore and Esteves 2004). Additionally, the assessment of the impact of UVR on natural phytoplankton assemblages was conducted before in this area (Barbieri et al. 2002; Villafañe et al. 2004; Helbling et al. 2005), however, using natural exposures and larger time intervals between sampling.

To evaluate the variations in UVR-induced photoinhibition of phytoplankton assemblages, routine sampling for experimentation was carried out every 2–3 days. Surface water samples were collected (ca. 100 m offshore) at mid morning using an acid-cleaned (1 N HCl) dark container and immediately taken to Estación de Fotobiología Playa Unión (EFPU; 5 min away from the sampling site) where the short-term effects of UVR upon phytoplankton photosynthetic rates were determined.

Experimentation

Samples were dispensed in 50-ml quartz tubes and inoculated with 5 μ Ci (0.185 MBq) of labeled sodium bicarbonate. The tubes were then attached to a black aluminum frame that was placed in a water bath inside a temperature-controlled environmental chamber (20°C). The samples were exposed for 2 h under a solar simulator (Hönle, Sol 1200, Germany). Three different radiation treatments (duplicate samples for each treatment) were implemented: (1) PAB treatment: samples receiving PAR + UV-A + UV-B (280–700 nm, unwrapped quartz

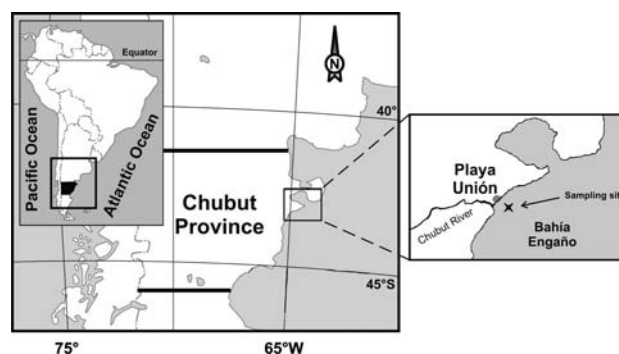


Fig. 1 Map showing the study area and the relative position of the Chubut Province in South America

tubes); (2) PA treatment: samples receiving PAR + UV-A (315–700 nm), tubes covered with Folex UV cut-off filter (Montagefolie, No. 10155099), and (3) P treatment: samples receiving only PAR (400–700 nm), tubes wrapped with Ultraphan UV Opak Digefra film [the transmission characteristics of filters and materials were previously reported elsewhere (Villafañe et al. 2003)]. The lamp was covered with acetate film to avoid UV-C exposure of the samples. The irradiances used in the experiments were 183, 69.9, and 1.7 W m⁻² for PAR, UV-A, and UV-B, respectively. It should be noted that PAR irradiance is lower and UVR levels are slightly higher than the mean noon solar irradiances during the experimentation period (see “Results”); however, they were within the upper and lower limits of irradiances measured during the experimental period. After the incubation period, the samples were filtered onto Whatman GF/F filters (25 mm in diameter) and the filters were exposed to HCl fumes overnight. Then, the filters were dried and counted using a liquid scintillation counter (Holm-Hansen and Helbling 1995). Photosynthetic inhibition for each wavelength interval (i.e., carbon fixation in the PAB and PA treatments relative to that in the P control) over the incubation period was calculated as follows:

$$\text{UV-B inhibition} = [(C_P - C_{PAB}) - (C_P - C_{PA})] / (C_P) \times 100$$

$$\text{UV-A inhibition} = (C_P - C_{PA}) / (C_P) \times 100$$

where C_P , C_{PA} , and C_{PAB} are the carbon fixation values in the P, PA, and PAB treatments, respectively.

Analyses and measurements

Pigment analyses

Duplicate aliquots of samples (100–250 ml) were filtered onto Whatman GF/F filters (25 mm in diameter) under dim light. The filters were immediately frozen in liquid nitrogen and stored at -80°C until analysis in The Netherlands. Filters were handled under dim light, freeze-dried (48 h), and pigments extracted in 4 ml of 90% cold acetone (v/v, 48 h, 5°C). Then, pigments were resolved using HPLC (Waters 2690 separation module, 996 photodiode array detector) with a C₁₈ 5 μm DeltaPak reversed-phase column (Milford, MA, USA) and identified by retention time and diode array spectroscopy (Van Leeuwe et al. 2006). Quantification was done using standard dilutions of chlorophyll a, b, fucoxanthin, diadinoxanthin, diatoxanthin, zeaxanthin, lutein, antheraxanthin, prasinolaxanthin, alloxanthin, peridinin, and violaxanthin. The CHEMTAX matrix factorization program (Mackey et al. 1996) was used to assess phytoplankton class abundances. The initial ratio matrix was largely based on the Southern Ocean

synthetic data set as presented by Mackey et al. (1997) using peridinin (dinoflagellates), fucoxanthin (diatoms), alloxanthin (cryptophytes), lutein (chlorophytes), and zeaxanthin (chlorophytes and cyanobacteria) as marker pigments. Prasinophytes might have been present in the samples, despite the absence of prasinolaxanthin in our samples, since not all prasinophytes contain this group-specific pigment. Yet, microscopy did not indicate the presence of prasinophyte: in contrast, coccoid green algae were observed more often in the area. Therefore, only chlorophytes were included in the calculations. For all phytoplankton classes, the ratio limits were set to 10% so that only little variability was allowed for the output ratio matrix.

Chlorophyll (chl a) concentration was measured twice, once for pigment fingerprinting (as described before) and once for calculations of carbon assimilation and size fractionation, using fluorometry. For this later analysis, duplicate aliquots of 100 ml of sample were filtered onto a Whatman GF/F filter (25 mm in diameter) and the photosynthetic pigments extracted in absolute methanol (7 ml for at least 1 h). The chl a concentration was calculated from the fluorescence of the extract, before and after acidification, using a fluorometer (Turner Designs model TD 700) (Holm-Hansen et al. 1965). Size fractionation was done by prefiltering a sample with a Nitex[®] mesh (20 μm pore size) with subsequent chl a analyses as described above; in this way, we had information of the total chl a concentration as well as on the chl a concentration in the $<20 \mu\text{m}$ size fraction. The fluorometer is routinely calibrated using pure chl a from *Anacystis nidulans* (Sigma C6144). As expected, HPLC-derived chl a concentration and fluorometer-derived chl a data were highly correlated ($R^2 = 0.9$, $P < 0.0001$, data not shown).

Additionally, scans of the methanolic extracts were obtained using a spectrophotometer (Hewlett Packard model HP 8453E) to estimate the amount of UV-absorbing compounds based on the peak at 337 nm (Helbling et al. 1996).

Taxonomic analyses

Samples for identification and enumeration of phytoplankton were placed in 125 ml brown bottles and fixed with buffered formalin (final concentration 0.4% of formaldehyde). A variable amount of sample (10–25 ml) was allowed to settle for 24 h in a Utermöhl chamber (Hydro-Bios GmbH, Germany) and species were enumerated and identified using an inverted microscope (Leica model DM IL) following the technique described by Villafañe and Reid (1995).

Atmospheric variables

Incident solar radiation over the study area was measured continuously using a broad band ELDONET radiometer (Real Time Computers Inc., Germany) that measures UV-B (280–315 nm), UV-A (315–400 nm), and PAR (400–700 nm) with a frequency of one reading per second and stored the minute-averaged value for each channel. In addition, continuous monitoring of other atmospheric variables (i.e., temperature, humidity, wind speed, and direction) was carried out using a meteorological station (Oregon Scientific model WMR-918). Total ozone column concentrations were obtained from NASA (<http://jwocky.gsfc.nasa.gov>).

Statistics

The data were reported either as mean and half-range (as duplicate samples were incubated due to the effective area under the solar simulator) or as mean and standard deviations when triplicate analyses were performed; the nonparametric Kruskal–Wallis test (Zar 1999) was used to test for significant differences between the samples exposed to different radiation treatments, using a 95% confidence limit.

We used multiple linear regression analysis to explain the variability observed in photosynthetic performance and UVR-induced photoinhibition. The variables that accounted for most of the variability were temperature, xanthophylls cycling, solar radiation, and species abundance (as determined by CHEMTAX analysis).

Results

Atmospheric variables

Solar radiation during the sampling period showed a day-to-day variability in the daily doses due to cloud cover; nevertheless, there was a trend for decreasing radiation values after Julian day 29 (Fig. 2a, b). During the study period, daily doses for PAR and UV-A (Fig. 2a) varied between 6,200 and 11,200 and 960–1730 kJ m^{-2} , respectively. Following the same trend, daily doses of UV-B ranged between 24.5 and 46.4 kJ m^{-2} , with low values determined on Julian days 35 and 36 (Fig. 2b). The mean noon irradiances for the period were 311 (SD = 72.3), 49.4 (SD = 10.5), and 1.55 (SD = 0.3) W m^{-2} for PAR, UV-A, and UV-B, respectively (data not shown). Ozone values over Bahía Engaño were variable, but generally high, ranging from 239 to 323 Dobson Units (D.U.) during January and February (Fig. 2b). Ambient air temperature

varied between 14.3 and 27.9°C, with a mean value of 19.4°C (Fig. 2c).

Pigments composition

Chl a concentration (Fig. 3a) during most of the study period had values ranging between 5 and 15 $\mu\text{g chl a l}^{-1}$. By the end of February, however, chl a concentration increased and reached values as high as 35 $\mu\text{g chl a l}^{-1}$. The samples were generally dominated by pico-nano-plankton cells (<20 μm) with more than 50% of chl a allocated in this fraction (Fig. 3a). Chl b, characteristic of green algae, showed small peaks during mid January (0.82 $\mu\text{g chl b l}^{-1}$) and at the beginning of February (2.1 $\mu\text{g chl b l}^{-1}$) (Fig. 3b). Zeaxanthin concentration varied between 0.19 and 0.72 $\mu\text{g l}^{-1}$, whereas lutein reached a maximum concentration of 0.35 $\mu\text{g l}^{-1}$ (Fig. 3c). Finally, fucoxanthin, diadinoxanthin, and diatoxanthin concentrations were generally low (<4 $\mu\text{g l}^{-1}$), but they increased towards the end of the sampling period, reaching values as high as 15.7, 2.76, and 1.14 $\mu\text{g l}^{-1}$, respectively (Fig. 3d).

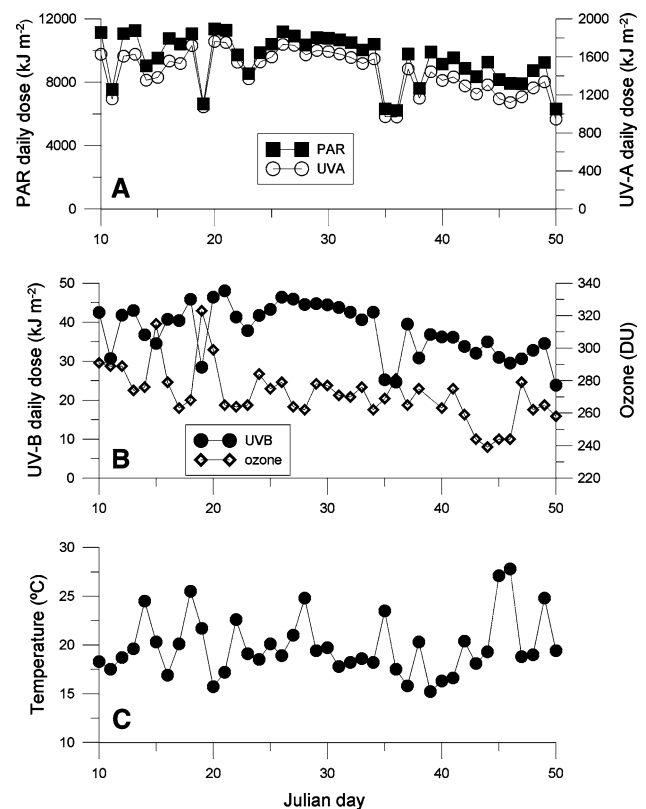


Fig. 2 Solar radiation, ozone and temperature during the study period. **a** Daily doses of photosynthetically active radiation (PAR, 400–700 nm) and UV-A (315–400 nm) in kJ m^{-2} ; **b** Daily doses of UV-B (280–315 nm) and total ozone column concentrations (in Dobson Units, D.U.) over Playa Unión and **c** Mean daily ambient temperature (°C)

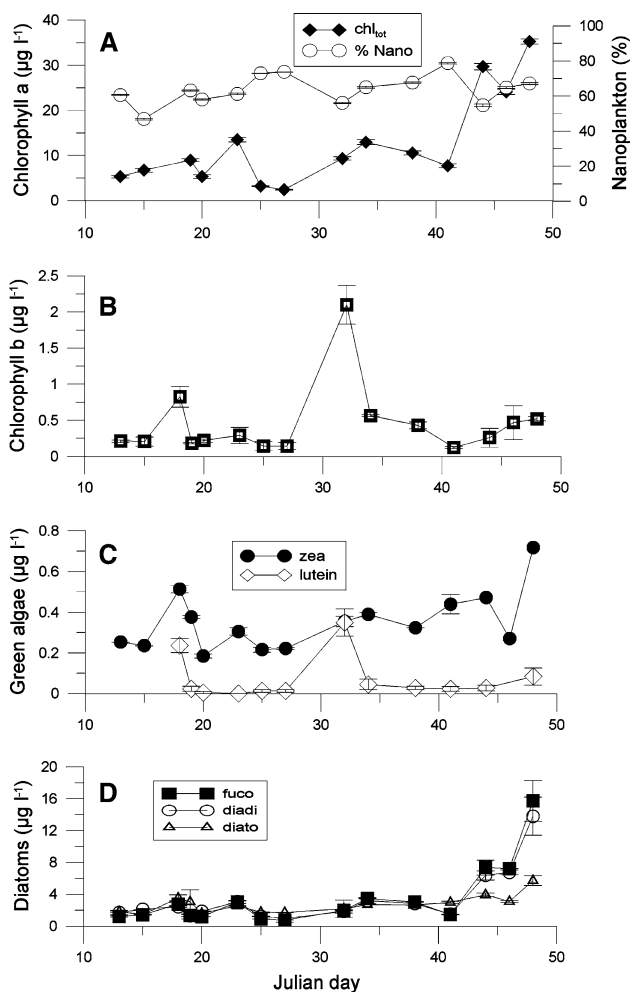


Fig. 3 Total concentration of pigments (in µg l⁻¹) throughout the study period. **a** Chl a and percentage of chl a in the nanoplankton fraction (<20 µm); **b** chlorophyll b; **c** zeaxanthin and lutein; **d** fucoxanthin, diadinoxanthin, and diatoxanthin. The vertical lines on top of the symbols indicate the half range

Taxonomic composition

There was a general good agreement between CHEMTAX data and microscopic determinations of species composition. There was large variability in the relative proportion of phytoplankton class abundances over the study period as assessed with the CHEMTAX program (Fig. 4a). Dinoflagellates as well as cryptophytes abundances were low during the study period, ranging between 0.01 and 5.4% and between 0.1 and 7.4% of total biomass, respectively. Chlorophytes and cyanobacteria (*Synechococcus* type) also showed high variability during the study period, ranging from 3.7 to 51.4% and from 4.8 to 29.8% of total biomass, respectively. Diatoms were found to be the most abundant group, ranging from 35.8% (on Julian day 32) to 88.5% (on Julian day 46) of total phytoplankton biomass. Phytoplankton abundance in terms of cell numbers (Fig. 4b) was

also variable, with values ranging between 223 and 2725 cells ml⁻¹, with a clear peak on Julian day 23, and also high values towards the end of the study period. The abundance of microplankton cells (>20 µm) was generally low (<200 cells ml⁻¹), but small peaks in cell numbers were determined on Julian days 23 and 44 with 225 and 434 cells ml⁻¹, respectively. Microscopic analysis revealed the conspicuous presence of picoplankton (including *Synechococcus* like cells) throughout the study period (Fig. 4c) with concentrations as high as 1,550 cells ml⁻¹. The high diatom concentrations were due to the presence of small (<20 µm) *Thalassiosira* species, although *Odontella aurita* and *Chaetoceros* spp. also contributed for an important part to total diatom abundance. The cell densities of dinoflagellates were always low, with few species represented in the samples such as *Gymnodinium* sp., *Protoperidinium* sp., and *Prorocentrum micans*.

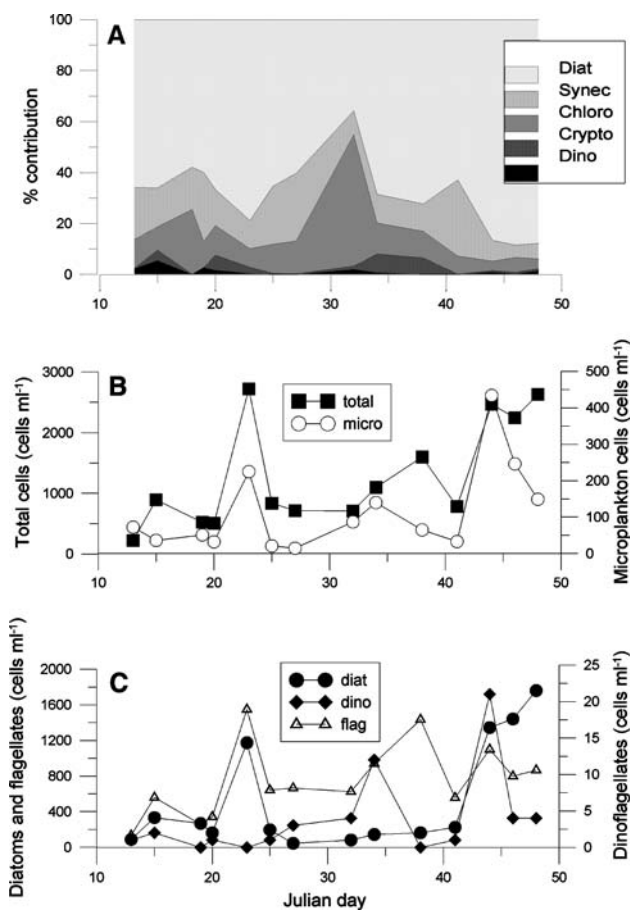


Fig. 4 Taxonomic composition of the phytoplankton assemblages throughout summer 2006. **a** Percent contribution of the major groups as resolved by CHEMTAX from the pigment data; **b** Total phytoplankton and microplankton (>20 µm) concentrations (in cells ml⁻¹) as assessed through microscopic analyses; and **c** diatoms, dinoflagellates, and flagellates concentration (in cells ml⁻¹) as determined by microscopic analyses; note the different scale (y axis) for dinoflagellates

UVR impact on carbon uptake

Assimilation numbers obtained during 2 h exposure to the solar simulator were variable and ranged between 4.4 and 10.4 $\mu\text{g C } (\mu\text{g chl a})^{-1} \text{ h}^{-1}$ in the P treatment (Fig. 5a). Lower assimilation numbers were found in samples receiving additionally UV-A and UV-B. Inhibition of photosynthesis (Fig. 5b) was detected in all samples, with UV-A and UV-B either contributing equally to the inhibition, or UV-B surpassing the contribution of UV-A. This latter case was especially evident at the beginning of the experimental period (Julian day 15) with 39% inhibition due to UV-B and 21% due to UV-A.

Photoprotective compounds

The potential protective role of xanthophylls was evaluated by considering both the pool of these pigments as well as the de-epoxidation status (diatoxanthin relative

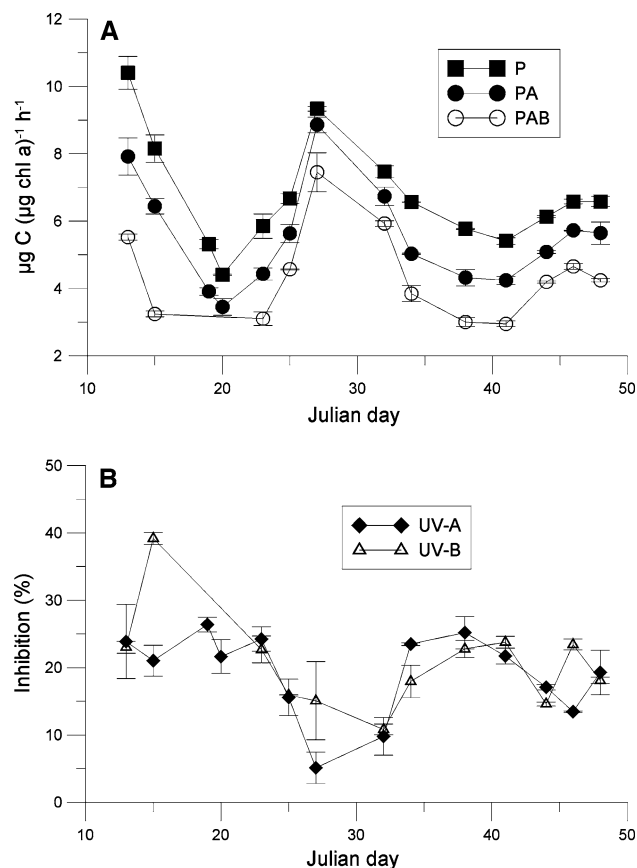


Fig. 5 **a** Phytoplankton assimilation numbers (in $\mu\text{C } (\mu\text{g chl a})^{-1} \text{ h}^{-1}$) throughout the study period for samples exposed to PAR only (P treatment), PAR + UV-A (PA treatment), and PAR + UV-A + UV-B (PAB treatment) (note that samples under the PAB treatment were lost on Julian days 19 and 20); **b** Percentage inhibition of carbon fixation due to UV-A and UV-B. The lines on top of the symbols indicate the half range

to diadinoxanthin + diatoxanthin— $dt/(dt + dd)$ (Fig. 6). Xanthophyll cycling of chlorophytes (VAZ cycle) could not be calculated due to the fact that only traces of violaxanthin and antheraxanthin were detected in the HPLC chromatograms. The total pool of xanthophylls ($dt + dd$) was normalized to diatom (as the dominant $dd + dt$ -containing group) chl a, calculated from the fuco/chl a ratio used in the CHEMTAX input matrix. This derived ratio ($(dd + dt)/\text{chl-a}$) was relatively high and ranged between 0.11 and 0.32. The extent of conversion of diadinoxanthin to diatoxanthin— $dt/(dt + dd)$ —throughout the study period was also relatively high with a mean value of 0.5 (SD = 0.12) and ranging between 0.29 and 0.69.

Variability of photosynthetic efficiency and UVR-induced photoinhibition

The relative contribution of the main factors accounting for most of the variability observed in the photosynthetic performance of PAR-exposed samples was done using a multiple linear regression analysis. The best model obtained ($R^2 = 0.97$, $P < 0.0001$) for the variability of assimilation numbers is shown in Fig. 7a, and it had the following equation:

$$P_{\text{ass}} = 0.073T - 2.733dt/(dt + dd) + 0.05E \quad (1)$$

where P_{ass} is the assimilation number of samples receiving only PAR, T is the ambient temperature, $dt/(dt + dd)$ is the rate of conversion of the xanthophylls cycle, and E is the solar radiation dosis.

For UVR-induced photoinhibition (UVR_{inh}), throughout the study period (Fig. 7b), we obtained the best model ($R^2 = 0.96$, $P < 0.0001$) as follows:

$$\text{UVR}_{\text{inh}} = 0.459 \text{ Diat} - 0.015 \text{ Chloro} + 5.246 \text{ Dino} + 0.78 \text{ Synech} + 2.151 \text{ Crypto} - 2.098 P_{\text{ass}} \quad (2)$$

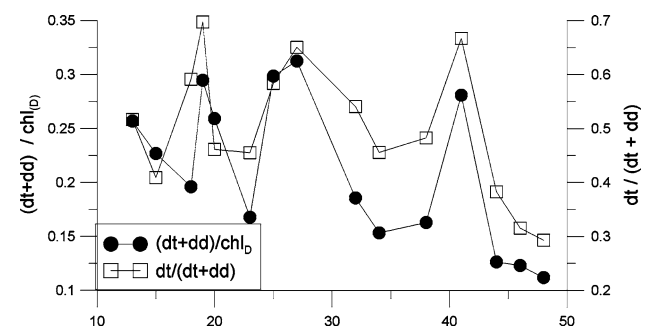


Fig. 6 Total pool of xanthophyll pigments, expressed as the sum of diadinoxanthin and diatoxanthin normalized to diatom chl a— $((dt + dd)/\text{chl } a_{(D)})$ —assuming a fucoxanthin to chl a ratio of 0.45 (Mackey et al. 1997) and the extent of conversion from diadinoxanthin to diatoxanthin $dt/(dt + dd)$ throughout the study period

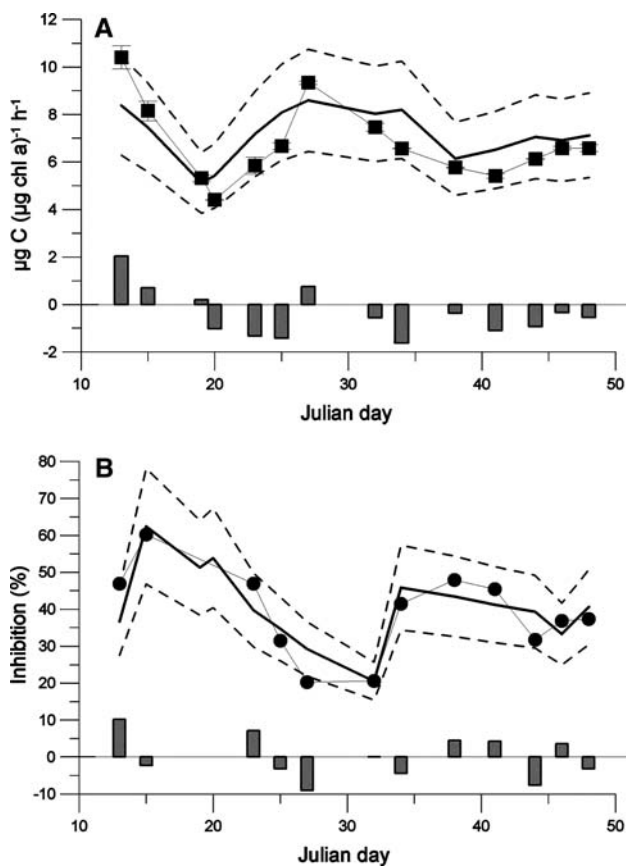


Fig. 7 Output from the multiple linear regression models as compared to the data obtained for the assimilation numbers for the PAR treatment in $\mu\text{C} (\mu\text{g chl a})^{-1} \text{h}^{-1}$ (a), and for UVR inhibition (b). The thin lines and symbols are the experimental data while the thick lines are the modeled data; the broken lines represent the 95% limit. The vertical bars in each panel are the residuals from the models

where Diat, Chloro, Dino, Synech, and Crypto are the contributions of diatoms, chlorophytes, dinoflagellates, *Synechococcus*, and cryptophytes (as determined by the CHEMTAX program, Fig. 4a) and P_{ass} is the assimilation number of samples receiving only PAR.

Discussion

In our study, we investigated the UVR-induced photoinhibition in relation to phytoplankton composition from Patagonian coastal waters. To complement our previous studies carried out in the area (Buma et al. 2001; Helbling et al. 2001; Villafañe et al. 2004), our approach here was to expose sea surface samples to constant temperature and UVR and PAR illumination. Thus, we focused on responses due to changes in community structure and their associated sensitivity to UVR. However, samples collected at different times during the study period had their light

history and environmental preacclimation that conditioned their overall UVR response. In the following paragraphs, we will discuss the variability observed in UVR-induced photoinhibition as associated to changes in taxonomic composition and other environmental variables.

Summer time is considered the postbloom condition in coastal Patagonian waters, with phytoplankton assemblages generally dominated by pico-nanoplankton cells ($<20 \mu\text{m}$) (Buma et al. 2001; Helbling et al. 2001; Barbieri et al. 2002; Villafañe et al. 2004). This dominance of pico-nanoplankton cells has been observed in Bahía Engaño throughout the study period, as seen in both chl a and cell abundances (Figs. 3, 4). We further determined that the pico-nanoplankton cells were mostly small diatoms, chlorophytes, and cyanobacteria (Fig. 4). This pico-nanoplankton abundance contrasts with the general pattern of dominance of microplankton species during the winter, where they cause blooms $>100 \mu\text{g chl a l}^{-1}$ (Barbieri et al. 2002; Villafañe et al. 1991, 2004). These blooms are associated with calm weather conditions during the winter that allow for the stratification of the water column. In contrast, the prevalence of high winds during spring and summer favor the occurrence of deep upper mixed layers that preclude the growth of large cells (Villafañe et al. 2004) as also seen in Antarctic waters (Kopczynska 1992). It should be noted that during summer 2006 wind speed was exceptionally low (daily mean during January 2006 = 2 m s^{-1}) as compared to the overall daily mean of 5 m s^{-1} that was previously reported for this period (Villafañe et al. 2004; Helbling et al. 2005). Although wind data for February 2006 were not available, qualitative observations allow generalizing on the calm weather conditions as determined during January. Wind has been found to be a key variable shaping plankton communities in the Patagonia region (Villafañe et al. 2004; Helbling et al. 2005; Gonçalves et al. 2007). Moreover, wind is also responsible for the amount of time that cells are exposed to high radiation levels (i.e., at or near surface waters). When calm conditions prevail, algae near the surface become high-light acclimated, whereas the opposite occurs when strong winds dominate. High-light acclimation in the diatom samples was supported by the high abundance of xanthophyll cycle pigments relative to chl a and by the relatively high conversion rates to diatoxanthin (mean = 0.5, Fig. 6). It has been previously determined that these compounds increase photoprotection during exposure to high PAR and UVR (Demers et al. 1991; Kudoh et al. 2003; Mohovic et al. 2006; van de Poll et al. 2006; Dimier et al. 2007).

The high assimilation numbers (Fig. 5a) as compared to those determined in an earlier study carried out in coastal Patagonian waters— $\sim 1 \mu\text{g C} (\mu\text{g chl a})^{-1} \text{h}^{-1}$ (Helbling et al. 2001)—suggest a better photosynthetic performance

of the phytoplankton assemblages sampled during the summer of 2006, even under the high radiation levels observed (Fig. 2). The high photosynthetic performance of phytoplankton during this period could be related to the input of nutrients via the outflow of the Chubut River. In fact and although we did not measure nutrient concentration during summer 2006, it has been shown previously (Helbling et al. 1992; Perez, personal communication) that the river carries a heavy load of nitrogen, phosphorus, and silicate due to supply of fertilizers used for agriculture upstream.

The multiple linear regression analysis indicated a positive relationship between temperature and assimilation number, which was expected due to the efficiency of enzymatic mechanisms (Falkowski 1981). In addition, a negative relation was observed between the rate of conversion of the xanthophyll cycle and assimilation numbers of PAR-exposed samples. The high conversion of xanthophylls to their heat-dissipating state suggests photosynthetic downregulation in these samples as a result of (previous) high light exposure, thereby depressing carbon incorporation rates while under the solar simulator. When cells were also exposed to UVR, they always displayed some degree of photoinhibition due to both UV-A and UV-B (Fig. 5). We observed high variability occurring in a relatively short period of time, with photoinhibition ranging between 5 and 26% and between 10 and 39% for UV-A and UV-B, respectively. These inhibition values are in the range as those previously reported for Patagonian coastal waters (Helbling et al. 2001; Helbling et al. 2005; Barbieri et al. 2002; Villafañe et al. 2004). Similar to assimilation numbers, multiple linear regressions analysis indicated that the variability in UVR-induced photoinhibition was significantly related to the contribution of diatoms, chlorophytes, dinoflagellates, *Synechococcus*, and cryptophytes in the samples and to the assimilation number of samples receiving only PAR. Furthermore, the negative relationship of P_{ass} and $dt/(dt + dd)$ (Eq. 1) was also supported by the positive relationship between the amount of diatoms and the UVR_{inh} (Eq. 2), suggesting that when high-light acclimated diatoms dominated, the assimilation numbers decreased and photosynthesis was more inhibited by UVR. On the other hand, UVR_{inh} was negatively related to the amount of chlorophytes, suggesting that this group had a better performance under UVR exposure as compared to others present during the study period.

Moreover, mycosporine like aminoacids (MAAs) were not detected in significant amounts throughout the study period (data not shown). The lack of these compounds was expectable, as during summer, the size structure of the communities did not favor their accumulation, because their useful concentration would be too high and osmotically disadvantageous (Garcia-Pichel 1994).

In conclusion, we have found that phytoplankton communities from Patagonia were sensitive to UVR stress, although the extent of the inhibition varied during the summer. Taxonomic composition played a key role in explaining the observed variability in UVR-induced inhibition throughout the study period. Other environmental variables, such as wind and nutrient input by the Chubut River, presumably also played an important role conditioning the photosynthetic performance of cells and so their response to exposure to UVR.

Acknowledgments This work was supported by the United Nations—Global Environmental Fund (PNUD B-C-39), Agencia Nacional de Promoción Científica y Tecnológica—ANPCyT (PICT 2005-32034), NWO/MEERVOUD (Grant No. 836.01.040 to Buma), NWO/NAAP (Grant No. 851.20.015 to van de Poll), and Fundación Playa Unión. We thank E. Barbieri, R. Flores, and R. Gonçalves for their help during experiments. We also thank the comments and suggestions of two anonymous reviewers that helped us to improve this manuscript. This is contribution number 112 of the Estación de Fotobiología Playa Unión. The experiments comply with the current Argentinean laws.

References

- Banaszak AT (2003) Photoprotective physiological and biochemical responses of aquatic organisms. In: Helbling EW, Zagarese HE (eds) UV effects in aquatic organisms and ecosystems. The Royal Society of Chemistry, Cambridge, pp 329–356
- Banaszak AT, Neale PJ (2001) Ultraviolet radiation sensitivity of photosynthesis in phytoplankton from an estuarine environment. *Limnol Oceanogr* 46:592–603
- Barbieri ES, Villafañe VE, Helbling EW (2002) Experimental assessment of UV effects upon temperate marine phytoplankton when exposed to variable radiation regimes. *Limnol Oceanogr* 47:1648–1655
- Bouchard JN, Campbell DA, Roy S (2005) Effects of UV-B radiation on the D1 protein cycle of natural phytoplankton communities from three latitudes (Canada, Brazil and Argentina). *J Phycol* 41:273–286. doi:10.1111/j.1529-8817.2005.04126.x
- Buma AGJ, Boelen P, Jeffrey WH (2003) UVR-induced DNA damage in aquatic organisms. In: Helbling EW, Zagarese HE (eds) UV effects in aquatic organisms and ecosystems. The Royal Society of Chemistry, Cambridge, pp 291–327
- Buma AGJ, Helbling EW, de Boer MK, Villafañe VE (2001) Patterns of DNA damage and photoinhibition in temperate South-Atlantic picophytoplankton exposed to solar ultraviolet radiation. *J Photochem Photobiol B Biol* 62:9–18. doi:10.1016/S1011-1344(01)00156-7
- Commendatore M, Esteves JL (2004) Natural and anthropogenic hydrocarbons in sediments from the Chubut River (Patagonia, Argentina). *Mar Pollut Bull* 48:910–918. doi:10.1016/j.marpolbul.2003.11.015
- Demers S, Roy S, Gagnon R, Vignault C (1991) Rapid light-induced changes in cell fluorescence and in xanthophyll-cycle pigments of *Alexandrium excavatum* (Dinophyceae) and *Thalassiosira pseudonana* (Bacillariophyceae): a photo-protection mechanism. *Mar Ecol Prog Ser* 76:185–193. doi:10.3354/meps076185
- Demming-Adams B (1990) Carotenoids and photoprotection in plants: a role for the carotenoid zeaxanthin. *Biochim Biophys Acta* 1020:1–24. doi:10.1016/0005-2728(90)90088-L

- Dimier C, Corato F, Tramontano F, Brunet C (2007) Photoprotection and xanthophyll-cycle activity in three marine diatoms. *J Phycol* 43:937–947. doi:10.1111/j.1529-8817.2007.00381.x
- Falkowski PG (1981) Light shade adaptation and assimilation numbers. *J Plankton Res* 3(2):203–216. doi:10.1093/plankt/3.2.203
- Furgal JA, Smith REH (1997) Ultraviolet radiation and photosynthesis by Georgian Bay phytoplankton of varying nutrient and photoadaptive status. *Can J Fish Aquat Sci* 54:1659–1667. doi:10.1139/cjfas-54-7-1659
- Gao K, Li G, Helbling EW, Villafañe VE (2007) Variability of UVR effects on photosynthesis of summer phytoplankton assemblages from a tropical coastal area of the South China Sea. *Photochem Photobiol* 83:802–809
- García-Pichel F (1994) A model for internal self-shading in planktonic organisms and its implications for the usefulness of ultraviolet sunscreens. *Limnol Oceanogr* 39:1704–1717
- Gonçalves RJ, Barbieri EB, Villafañe VE, Helbling EW (2007) Motility of *Daphnia spinulata* as affected by solar radiation throughout an annual cycle in mid-latitudes of Patagonia. *Photochem Photobiol* 83:824–832
- Häder DP, Kumar HD, Smith RC, Worrest RC (2007) Effects of solar UV radiation on aquatic ecosystems and interactions with climate change. *Photochem Photobiol Sci* 6:267–285. doi:10.1039/b700020k
- Helbling EW, Barbieri ES, Marcoval MA, Gonçalves RJ, Villafañe VE (2005) Impact of solar ultraviolet radiation on marine phytoplankton of Patagonia, Argentina. *Photochem Photobiol* 81:807–818. doi:10.1562/2005-03-02-RA-452R.1
- Helbling EW, Buma AGJ, de Boer MK, Villafañe VE (2001) In situ impact of solar ultraviolet radiation on photosynthesis and DNA in temperate marine phytoplankton. *Mar Ecol Prog Ser* 211:43–49. doi:10.3354/meps211043
- Helbling EW, Chalker BE, Dunlap WC, Holm-Hansen O, Villafañe VE (1996) Photoacclimation of antarctic marine diatoms to solar ultraviolet radiation. *J Exp Mar Biol Ecol* 204:85–101. doi:10.1016/0022-0981(96)02591-9
- Helbling EW, Santamarina JM, Villafañe VE (1992) Chubut river estuary (Argentina): estuarine variability under different conditions of river discharge. *Rev Biol Mar* 27:73–90
- Holm-Hansen O, Helbling EW (1995) Técnicas para la medición de la productividad primaria en el fitoplancton. In: Alveal K, Ferrario ME, Oliveira EC, Sar E (eds) *Manual de Métodos Ficológicos*. Universidad de Concepción, Concepción, pp 329–350
- Holm-Hansen O, Lorenzen CJ, Holmes RW, Strickland JDH (1965) Fluorometric determination of chlorophyll. *J Cons Permanent Int pour l' Explor de la Mer* 30:3–15
- Kopczynska EE (1992) Dominance of microflagellates over diatoms in the Antarctic areas of deep vertical mixing and krill concentrations. *J Plankton Res* 14(8):1031–1054. doi:10.1093/plankt/14.8.1031
- Kudoh S, Imura S, Kashino Y (2003) Xanthophyll-cycle of ice algae on the sea ice bottom in Saroma Ko lagoon, Hokkaido, Japan. *Polar Biosci* 16:86–97
- Mackey MD, Higgins HW, Mackey D, Wright S (1997) CHEMTAX users manual: a program for estimating class abundances from chemical markers: application to HPLC measurements of phytoplankton pigments. CSIRO Marine Laboratories Report 229, Hobart, 42 pp
- Mackey MD, Mackey DJ, Higgins HW, Wright SW (1996) CHEMTAX—a program for estimating class abundances from chemical markers: Application to HPLC measurements of phytoplankton. *Mar Ecol Prog Ser* 144:265–283. doi:10.3354/meps144265
- Marcoval MA, Villafañe VE, Helbling EW (2007) Interactive effects of ultraviolet radiation and nutrient addition on growth and photosynthesis performance of four species of marine phytoplankton. *J Photochem Photobiol B Biol* 89:78–87. doi:10.1016/j.jphotobiol.2007.09.004
- Mohovic B, Ganesella SMF, Laurion I, Roy S (2006) Ultraviolet-B photoprotection efficiency of mesocosm-enclosed natural phytoplankton communities from different latitudes: Rimouski (Canada) and Ubatuba (Brazil). *Photochem Photobiol* 82:952–961. doi:10.1562/2005-09-30-RA-707
- Perillo GME, Piccolo MC, Scapini MC, Orfila J (1989) Hydrography and circulation of the Chubut river estuary (Argentina). *Estuaries* 12(3):186–194. doi:10.2307/1351823
- Richter P, Häder DP, Gonçalves RJ, Marcoval MA, Villafañe VE, Helbling EW (2007) Vertical migration and motility responses in three marine phytoplankton species exposed to solar radiation. *Photochem Photobiol* 83:810–817
- Roy S (2000) Strategies for the minimization of UV-induced damage. In: De Mora SJ, Demers S, Vernet M (eds) *The effects of UV radiation in the marine environment*. Cambridge University Press, Cambridge, pp 177–205
- Sastre AV, Santinelli NH, Otaño SH, Ivanissevich ME, Ayestarán MG (1994) Diatom blooms and their relation to water supply. *Verh Int Ver Theor Angew Limnol* 25:1974–1978
- Sobrino C, Neale PJ, Montero O, Lubián LM (2005) Biological weighting function for xanthophyll de-epoxidation induced by ultraviolet radiation. *Physiol Plant* 125:41–51. doi:10.1111/j.1399-3054.2005.00538.x
- van de Poll WH, Alderkamp A-C, Janknegt PJ (2006) Photoacclimation modulates excessive photosynthetically active and ultraviolet radiation effects in a temperate and an Antarctic marine diatom. *Limnol Oceanogr* 51:1239–1248
- Van Leeuwe MA, Villerius LA, Roggeveld J, Visser RJW, Stefels J (2006) An optimized method for automated analysis of algal pigments by HPLC. *Mar Chem* 102:267–275. doi:10.1016/j.marchem.2006.05.003
- Vernet M (2000) Effects of UV radiation on the physiology and ecology of marine phytoplankton. In: de Mora S, Demers S, Vernet M (eds) *The effects of UV radiation in the marine environment*. Cambridge University Press, Cambridge, pp 237–278
- Villafañe VE, Barbieri ES, Helbling EW (2004) Annual patterns of ultraviolet radiation effects on temperate marine phytoplankton off Patagonia, Argentina. *J Plankton Res* 26:167–174. doi:10.1093/plankt/fbh011
- Villafañe VE, Helbling EW, Santamarina J (1991) Phytoplankton blooms in the Chubut river estuary (Argentina): Influence of stratification and salinity. *Rev Biol Mar* 26:1–20
- Villafañe VE, Reid FMH (1995) Métodos de microscopía para la cuantificación del fitoplancton. In: Alveal K, Ferrario ME, Oliveira EC, Sar E (eds) *Manual de Métodos Ficológicos*. Universidad de Concepción, Concepción, pp 169–185
- Villafañe VE, Sundbäck K, Figueroa FL, Helbling EW (2003) Photosynthesis in the aquatic environment as affected by UVR. In: Helbling EW, Zagarese HE (eds) *UV effects in aquatic organisms and ecosystems*. Royal Society of Chemistry, Cambridge, pp 357–397
- Zar JH (1999) *Biostatistical analysis*. Prentice Hall, Englewood Cliffs